The influence of interlayer/epoxy adhesion on the mode-I and mode-II fracture response of carbon fibre/epoxy composites interleaved with thermoplastic veils

Quan, Dong; Deegan, Brian; Alderliesten, René; Dransfeld, Clemens; Murphy, Neal; Ivanković, Alojz; Benedictus, Rinze

DOI
10.1016/j.matdes.2020.108781

Publication date
2020

Document Version
Final published version

Published in
Materials and Design

Citation (APA)
Quan, D., Deegan, B., Alderliesten, R., Dransfeld, C., Murphy, N., Ivanković, A., & Benedictus, R. (2020). The influence of interlayer/epoxy adhesion on the mode-I and mode-II fracture response of carbon fibre/epoxy composites interleaved with thermoplastic veils. *Materials and Design*, *192*, Article 108781. https://doi.org/10.1016/j.matdes.2020.108781

Materials and Design 192 (2020) 108781

Contents lists available at ScienceDirect

Materials and Design

journal homepage: www.elsevier.com/locate/matdes

The influence of interlayer/epoxy adhesion on the mode-I and mode-II fracture response of carbon fibre/epoxy composites interleaved with thermoplastic veils

Dong Quan [a,*], Brian Deegan [b], René Alderliesten [a], Clemens Dransfeld [a], Neal Murphy [c], Alojz Ivanković [c], Rinze Benedictus [a]

[a] Department of Aerospace Structures and Materials, Delft University of Technology, Netherlands
[b] Adhesives Research, Henkel Ireland Operations & Research Ltd., Ireland
[c] School of Mechanical and Materials Engineering, University College Dublin, Ireland

HIGHLIGHTS

- A UV-irradiation method was proposed for the surface functionalisation of PPS veils.
- The veil/epoxy adhesion had been significantly improved upon the UV-treatment.
- The effects of the veil/epoxy adhesion on the fracture behaviour of interleaved laminates were studied.
- The toughening performance and mechanisms of the PPS veils were significantly affected by the UV-treatment.

GRAPHICAL ABSTRACT

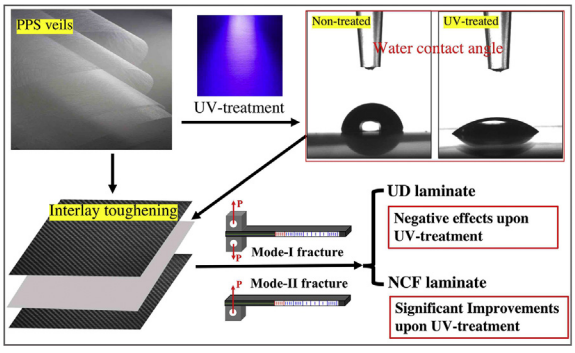

ARTICLE INFO

Article history:
Received 6 April 2020
Received in revised form 1 May 2020
Accepted 2 May 2020
Available online 7 May 2020

Keywords:
Polymer-matrix composites
Interlay toughening
Thermoplastic veils
Interlayer/matrix adhesion
Fracture toughness

ABSTRACT

The compatibility between the majority of thermoplastic veils (TPVs) and epoxies is typically poor, owing to the inherently low surface energies of thermoplastics. This tends to largely affect the toughening performance of TPVs as interlayer materials of carbon fibre/epoxy composites. The traditional methods for surface activation of thermoplastics, such as corona discharge, plasma treatment and acid etches, are not applicable to TPVs as they could cause significant damage to the thermoplastic fibres with nano-/micro-scale diameters. Herein, a UV-irradiation technique was proposed to active the surfaces of polyphenylene-sulfide (PPS) veils, that effectively improved their adhesion with epoxies. Consequently, the effects of an improved veil/epoxy adhesion on the mode-I and mode-II fracture behaviour and corresponding fracture mechanisms of the interleaved laminates were investigated. It was found that an improved veil/epoxy adhesion significantly enhanced the toughening performance of the PPS veils for the laminates manufactured by resin transfer moulding of non-crimp fabrics, by introducing additional carbon fibre delamination and significant PPS fibre damage during the fracture process. In contrast, the increased level of veil/epoxy adhesion inhibited PPS fibre bridging during the fracture process of

* Corresponding author.
E-mail address: d.quan-1@tudelft.nl (D. Quan).

https://doi.org/10.1016/j.matdes.2020.108781

the laminates produced from unidirectional prepregs, and caused considerable adverse effects on the fracture performance.

1. Introduction

Carbon fibre reinforced polymers (CFRPs) are widely used in multiple industries, including aerospace, automotive and marine sectors, because of their outstanding structural performance and light weight. One of the major disadvantages of CFPRs is that they are prone to interply delamination due to their laminated structure. Accordingly, extensive research has been carried out over the last two decades in an effort to improve the interlaminar fracture toughness of CFRPs. The application of thermoplastic veils as interlayer materials of CFRPs is attracting considerable attention from both academics and industrialists [1], due to the fact that it can significantly enhance the interlaminar fracture toughness of CFRPs [1–8], without causing detrimental effects to the other mechanical properties, such as flexural modulus and strength [2,9–11], and interlaminar shear strength [2–4,10]. This is attributed to the tough, ductile, porous and lightweight nature of the thermoplastic veils.

A large number of studies investigated the influencing factors on the toughening performance of thermoplastic veils, with main focus on the areal density of the veils [2,3,12–14], the veil material [7,12,15,16], the form of the veils in the FRPs, i.e. melted or non-melted [7,9], and the architecture of the carbon fibre fabrics [8,14–16]. While the effects of these factors were proven to be critical, the toughening efficiency of thermoplastic veils as interlayer materials of CFRPs is still not conclusively interpreted and predictable. This is due to the significantly varied results between different studies. For example, as reviewed in [1,17,18], the maximum increases in the mode-I and mode-II fracture energies of the unidirectional (UD) laminates upon interlaying thermoplastic veils was observed to be above 200% in [3,14,18–20], and this value dropped to below 50% in [7,12,21,22], and even worse, adverse effects were observed in some other publications, including [11,13–15]. Clearly, it is important to fully understand the reasons for these significant variations, but has not been achieved yet. The level of the adhesion between thermoplastic veils and epoxy matrix is another critical factor that tends to significantly affect the toughening performance of the veils. However, to date, there is still a lack of studies on the effects of thermoplastic veils/epoxy adhesion on the mechanical, fracture and impact response of interleaved laminates, mainly due to the lack of proper techniques to improve the veils/epoxy adhesion. It should be noted that the level of the adhesion between the majority of thermoplastic veils and epoxies is typically poor, owing to the inherently low reactivity, low surface energies and weak polarities of those thermoplastics [23]. For example, in references [15, 24–26] and our previous studies [18,19], it was observed that the thermoplastic fibres possessed very smooth surfaces (without epoxy attached to them) and exhibited no visible damage to the fibres themselves after they were pulled-out from the epoxy matrix during the fracture process of the interleaved laminates. This clearly demonstrated a poor interaction between the veils and the epoxy during the fracture process. The foremost challenge for improving the thermoplastic veil/epoxy adhesion is that traditional surface treatment methods for thermoplastic materials, such as corona discharge, plasma treatment, acid etches and oxidising flame treatment are not applicable to thermoplastic veils. This is because of these methods could cause significant damage to the thermoplastic fibres who possessed micro-/nano-scale diameters. Ultraviolet light (UV)-irradiation was initiatlly employed to remove organic contaminants on the surfaces of polymers [27], and then it proved to effectively enhance the adhesion at the interface of dissimilar materials, such as copper/epoxy [28], PMMA/gold [29] and silicon/gold [30]. Recently, Shi et al. [31] used polyether-ether-ketone (PEEK) films as adhesives for co-cure joining of carbon fibre/epoxy composite. It was observed that the application of the UV-irradiation to the PEEK films significantly improved the mode-I fracture energy of the adhesive joints from none to 820 J/m^2. Obviously, the UV-irradiation method exhibited some promise as a surface preparation method of thermoplastic veils to enhance their adhesion with epoxies, and subsequently, it can facilitate investigations on the fracture behaviour of interleaved laminates with improved veil/epoxy adhesion. To the best knowledge of the authors, there is no relevant study in this filed yet.

The primary novelty of this work was that a UV-irradiation technique was proposed to active the surface of thermoplastic veils, that significantly improved the veil/epoxy adhesion, and subsequently allowed to investigate the effects of the veil/epoxy adhesion on the fracture behaviour of the CFRPs interleaved with thermoplastic veils. In particular, polyphenylene-sulfide (PPS) veils with different areal densities were UV-irradiated for a short time, and then used to interlay two types of aerospace-grade CFRPs produced from UD prepregs and resin transfer moulding (RTM) of non-crimp carbon fibre fabrics (NCFs). These two laminate systems were studied because of their non-modified laminates exhibited significantly different fracture properties and mechanisms, which subsequently affected the toughening levels and mechanisms of the non-treated thermoplastic veils [18,19]. The mode-I and mode-II fracture behaviour and corresponding fracture mechanisms of the laminates interleaved with UV-treated PPS veils were investigated. The results were compared with those of the laminates interleaved with non-treated PPS veils in [18,19], to obtain an understanding on the effects of the thermoplastic veil/epoxy adhesion.

2. Experimental

2.1. Materials

Two aerospace-grade CFRPs fabricated from UD carbon fibre/epoxy prepreg and RTM of NCFs were studied in this work. The UD carbon fibre prepreg was HYE-1034E from Cytec (Solvay Group), UK. The NCF was biaxial Toray T700Sc 50C from Saertex GmbH, Germany. The epoxy resin for RTM of the NCF laminates was CYCOM 890RTM from Cytec (Solvay Group), UK. Thermoplastic PPS veils with an areal density of 5, 10 and 15 g/m^2 were supplied by Technical Fibre Products Ltd., UK. In this paper, they are referred to as PPS5, PPS10 and PPS15, respectively. Additional information on these materials can be found in [19].

2.2. Processing and characterisation of the CFRPs

Surface activation of the PPS veils was performed in an in-house UV-irradiation system, equipped with a Light Hammer 6 UV source (Heraeus Noblelight, UK). The intensities of the UV spectral ranges were measured to be 371 mW/cm^2, 414 mW/cm^2, 141 mW/cm^2 and 23 mW/cm^2 for the UVV (395–445 nm), UVA (320–390 nm), UVB (280–320 nm) and UVC (250–260 nm), respectively, using a UV Power Puck from EIT Inc., USA. After the top side of the veil (facing the UV lamp) was treated for 10 s, the veil was inverted to treat its opposite side for another 10 s. To evaluate the effectiveness of the UV-treatment on the surface activation of the PPS veils, a sheet of PPS film (the same grade of PPS polymer as the veils) was also UV-irradiated by following the same procedure. The chemical composition of the non-treated and UV-treated PPS film surfaces were analysed using a X-ray photoelectron spectrometer (XPS, Kratos Axis Ultra DLD), equipped with Al Kα (1486.7 eV) X-ray source. The surface wettability of the PPS film was also investigated using an Attension Theta contact angle meter.

To manufacture the UD laminates, a hand layup process was used to prepare a layup consisting of 26 plies of UD carbon fibre prepregs and one layer of PPS veil at the mid-plane. The prepreg layup was consolidated under vacuum and ambient temperature for 45 min, and then cured within an in-house press-clave at 180 °C under a pressure of 0.5 MPa for 90 min. For the NCF laminates, a layup consisting of eight plies of dry carbon fibre fabrics with a stacking sequence of $[0/90]_{4S}$ and one layer of PPS veils between the 4th and 5th plies was prepared. The layup was sealed in an aluminium mould and then placed in the press-clave for a vacuum-assisted RTM process. The NCF laminates was also cured at 180 °C under a pressure of 0.5 MPa for 90 min. It should be noted that, during the layup procedure, a layer of PTFE film with a thickness of 12.5 μm was placed at the mid-plane at desired location to create crack starters in the fracture test specimens.

The mode-I and mode-II fracture behaviour of the interleaved laminates were studied using a double cantilever beam (DCB) test according to ISO15024 [32] and an end-loaded split (ELS) test according to ISO15114 [33], respectively. The tests were carried out using a Zwick/Roell ZO10 testing machine at a constant displacement rate of 2 mm/min and 1 mm/min for the DCB tests and the ELS tests, respectively. The length of the crack was monitored using a high resolution digital camera, and it was synchronised with the load and displacement measurements based on the start time of the test. A 5 mm long precrack from the crack starter was generated by loading the samples under an opening mode for both the DCB and the ELS specimens. A corrected beam theory analysis was used to evaluate the mode-I fracture energy, G_{IC} [32]:

$$G_{IC} = \frac{3P\delta}{2B(a+|\Delta|)} \cdot \frac{F}{N} \tag{1}$$

where P is the load, δ is the opening displacement, B is the width of the specimen, a is the crack length from the load line. F, N and Δ are the correction factors for large displacements, load block effects and root rotation of the crack tip, respectively. The mode-II fracture energy, G_{IIC} was determined based on the corrected beam theory using an effective crack length, as described in [33]:

$$G_{IIC} = \frac{9P^2a_e^2}{4B^2h^3E_1} \tag{2}$$

where h is half thickness of the specimen and E_1 is the flexural modulus of the specimen. a_e is the effective crack length, that was calculated as:

$$a_e = \left[\frac{1}{3}\left\{2BCh^3E_1 - (L+\Delta_{clamp})^3\right\}\right]^{\frac{1}{3}} \tag{3}$$

where C is the compliance of the ELS specimen, L is the free length of the specimen between the load-line and clamp, and Δ_{clamp} is the clamp correction factor. The crack initiation values for the mode-I and mode-II fracture energies were determined using the 5% offset approach according to [32,33]. However, this approach resulted in unrealistically high values for the mode-II crack initiation energy of the NCF laminates, and hence a non-linear point approach [33] was used for the NCF laminates. At least three replicate tests were conducted for each set. The fracture surfaces of the DCB and ELS specimens were imaged using an optical microscope (ZEISS Discovery V8) and a scanning electron microscope (SEM, JOEL JSM-7500F) to investigate the fracture mechanisms.

Table 1
Chemical composition of the surfaces of the PPS film before and after the UV-treatment.

TPCs	O 1s (%)	C 1s (%)	Ca 2p (%)	S 2p (%)	Si 2s (%)	Na 1s (%)	N 1s (%)
Non-treated	10.06	75.80	3.09	10.15	0.90	*	*
UV-treated	16.47	67.95	1.63	11.77	1.23	0.62	0.33

3. Results and discussion

3.1. Surface characterisation of the PPS polymer

Table 1 shows the chemical composition of the surfaces of the PPS film before and after the UV-treatment. It was found that the content of oxygen atoms on the PPS surfaces significantly increased from 10.06% to 16.47% upon applying the UV-irradiation to the PPS film. This was due to the breakage of the C—C/C—H bonds and following the generation of C—O, C═O and O—C═O species [34–36] on the surface of the PPS. The changes in the chemical composition significantly decreased the water contact angle from 79.7 ± 1.9° of the non-treated PPS surface to 43.0 ± 0.8° of the UV-irradiated PPS surface, as shown in Fig. 1. These observations clearly demonstrated that applying a short-time, i.e. 10 s, UV treatment to the PPS veils could effectively improve their surface activity. Consequently, it significantly increased the PPS veil/epoxy adhesion, which was confirmed by analysing the fracture surfaces of the interleaved laminates in Section 3.4.

3.2. Fracture behaviour of the interleaved NCF laminates

Fig. 2 shows representative mode-I R-curves from the DCB tests of the NCF laminates interleaved with original [19] and UV-treated PPS veils, and the corresponding fracture energies are summarised in Table 2. In this paper, the interleaved laminates were referred to as the type of the laminate system followed by the type of the interlayer material, e.g. UD/PPS5 represents the UD laminates interleaved non-treated PPS5 veils and UD/PPS5(UV) means the corresponding PPS5 veils were UV-treated. It was found that applying the UV-irradiation to the PPS veils significantly increased the mode-I crack initiation energy (G_{IC}^{ini}) of the interleaved NCF laminates. G_{IC}^{ini} was measured to be more or less the same for all the NCF laminates interleaved with UV-treated PPS veils, i.e. above 660 J/m^2 in all cases. These values were much higher than those of the counterparts containing original PPS veils, as shown in Table 2. A 'rising' R-curve behaviour was observed for all the NCF laminates. However, the 'rising' trend of the R-curves was less prominent for the laminates interleaved with UV-treated veils than those containing original veils, see Fig. 2. This typically indicates a reduction in the amount of fibre bridging during the fracture process, and resulted in a considerable drop in the values of ΔG_{IC} i.e. the difference between the mode-I crack propagation energy (G_{IC}^{prop}) and G_{IC}^{ini} [37] in all cases. For example, ΔG_{IC} decreased from 207 J/m^2 of the NCF/PPS5 laminate to 72 J/m^2 of the NCF/PPS5(UV) laminate upon the application of the UV-treatment to the PPS5 veils, as shown in Table 2. Another observation was that the effects of the areal density of the veils on G_{IC}^{prop} were less prominent for the UV-treated veils than the original PPS veils, i.e. as the areal density of the veils increased from 5 g/m^2 to 15/m^2, G_{IC}^{prop} notably increased from 599 J/m^2 to 823 J/m^2 (by 37%) for the laminates interleaved with original veils, and slightly increased from 734 J/m^2 to 799 J/m^2 (by 9%) for the laminates containing UV-treated veils. Fig. 3 shows representative photographs and light microscopy images of the fracture surfaces of the DCB specimens for the interleaved NCF laminates. It was observed that a large number of PPS fibres existed on both sides of the fracture surfaces in both cases, indicating a cohesive failure inside the PPS veil/epoxy layer during the mode-I fracture process. Moreover, strips of broken carbon

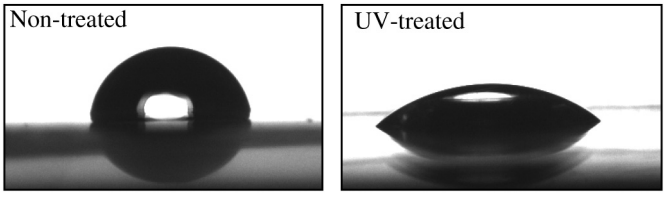

Fig. 1. The water drops on the surfaces of the non-treated and UV-treated PPS films.

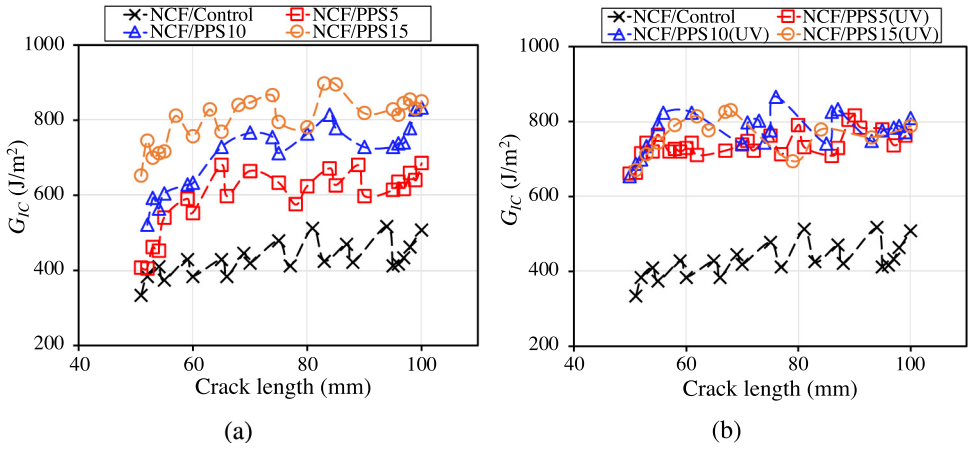

Fig. 2. Mode-I *R*-curves of the NCF laminates interleaved with (a) original [19] and (b) UV-treated PPS veils from the DCB tests.

fibres were observed on the fracture surfaces of the NCF/PPS10(UV) laminates, indicating the presence of additional carbon fibre delamination and associated carbon fibre bridging and breakage during the fracture process.

Fig. 4 shows representative *R*-curves from the ELS tests of the NCF laminates interleaved with original [18] and UV-irradiated PPS veils. The corresponding fracture energies are summarised in Table 2. The mode-II *R*-curves of the NCF control laminate exhibited a continuously 'rising' trend, as shown in Fig. 4. In this case, the last point on the *R*-curves, corresponding to the mode-II fracture energy at the instant of the dynamic failure of the ELS specimens, was taken as the mode-II fracture propagation energy (G_{IIC}^{prop}). For the other laminates, G_{IIC}^{prop} was taken as the average of all the values after the initial 'rising' stage of the *R*-curves, i.e. after a crack length of 75 mm for the NCF laminates interleaved with original PPS veils and after 85 mm for those containing UV-treated PPS veils, see Fig. 4. It was found that an improved veil/epoxy adhesion upon the UV-treatment significantly increased both of the mode-II crack initiation energy, G_{IIC}^{ini}, and mode-II crack propagation energy, G_{IIC}^{prop} of the interleaved NCF laminates. For example, G_{IIC}^{ini} increased from 1280 J/m^2, 1608 J/m^2 and 1925 J/m^2 for the NCF laminates interleaved with original PPS5, PPS10 and PPS15 veils to 2216 J/m^2 (by 73%), 2381 J/m^2 (by 48%) and 2996 J/m^2 (by 56%), respectively, due to the application of the UV-treatment to the veils. Similarly to the mode-I fracture energies, ΔG_{IIC}, which typically indicates the contribution of fibre bridging mechanism to the mode-II fracture energies, was smaller for the NCF laminates interleaved with UV-treated PPS veils, as shown in Table 2. Representative photographs and light microscopy images of the fracture surfaces of the ELS specimens for the interleaved NCF laminates are shown in Fig. 5. It was observed that the crack propagated cohesively in the PPS veil/epoxy layer for the non-treated veil interleaved NCF laminates, i.e. NCF/PPS10, leaving numerous PPS fibres on both sides of the fracture surfaces. The application of the UV-treatment to the PPS veils alternated the fracture mechanisms of the interleaved NCF laminates from a cohesive failure to a combination of cohesive failure within the veil/epoxy layer and carbon fibre delamination and bridging, evidenced by the presence of a few bundles of broken carbon fibres on the fracture surfaces of the NCF/PPS10(UV) laminates, see Fig. 5.

3.3. Fracture behaviour of the interleaved UD laminates

Representative mode-I *R*-curves from the DCB tests of the UD laminates interleaved with original PPS veils [19] and UV-irradiated PPS veils are shown in Fig. 6, and the corresponding fracture energies are summarised in Table 3. A comparison between Fig. 6(a) and (b) clearly shows that applying the UV-treatment to the PPS veils had little effects on G_{IC}^{ini} of the interleaved UD laminates. However, it considerably reduced the 'rising' trend of the *R*-curves, and subsequently resulted in a decrease in G_{IC}^{prop}, as shown in Table 3. For example, by applying the UV-treatment to the PPS veils, G_{IC}^{prop} decreased from 282 J/m^2, 368 J/m^2 and 542 J/m^2 of the original PPS5, PPS10 and PPS15 interleaved UD laminates to 222 J/m^2, 317 J/m^2 and 473 J/m^2, respectively. Correspondingly, the contribution of fibre bridging mechanisms to the energy consumption, i.e. ΔG_{IC}, was approximately halved in all these cases, as shown in Table 3. Representative photographs and microscopy images of the fracture surfaces of the DCB specimens of the UD laminates are shown in Fig. 7. It was found that the fracture surfaces of the UD/PPS10 and UD/PPS10(UV) laminates appeared more or less the same at these scales, i.e. both sides of the fracture surfaces were covered with numerous PPS fibres. This indicates that the crack propagated cohesively inside the PPS fibre/epoxy layer in both cases.

Table 2
Mode-I and mode-II fracture energies of the interleaved NCF laminates. $\Delta G = G^{prop} - G^{ini}$. Values in brackets indicate the percentage increases of the fracture energies over those of the corresponding control laminates.

Specimens	G_{IC}^{ini} (J/m^2)	G_{IC}^{prop} (J/m^2)	ΔG_{IC} (J/m^2)	G_{IIC}^{ini} (J/m^2)	G_{IIC}^{prop} (J/m^2)	ΔG_{IIC} (J/m^2)
NCF control	369 ± 28	463 ± 15	94	1185 ± 115	2549	1364
Original PPS veils						
NCF/PPS5	392 ± 40 (6%)	599 ± 31 (29%)	207	1280 ± 129 (8%)	2277 ± 150 (−11%)	997
NCF/PPS10	524 ± 59 (42%)	732 ± 31 (58%)	208	1608 ± 150 (36%)	2724 ± 72 (7%)	1116
NCF/PPS15	613 ± 9 (66%)	823 ± 28 (78%)	210	1925 ± 130 (62%)	2908 ± 142 (14%)	983
UV-treated PPS veils						
NCF/PPS5(UV)	662 ± 51 (79%)	734 ± 21 (59%)	72	2216 ± 234 (87%)	2844 ± 198 (12%)	628
NCF/PPS10(UV)	668 ± 33 (81%)	754 ± 40 (63%)	86	2381 ± 293 (101%)	3144 ± 350 (23%)	763
NCF/PPS15(UV)	681 ± 79 (85%)	799 ± 44 (73%)	118	2996 ± 145 (153%)	3807 ± 119 (49%)	811

asterisks mean none in this table, i.e. Na and N elements were not detected.

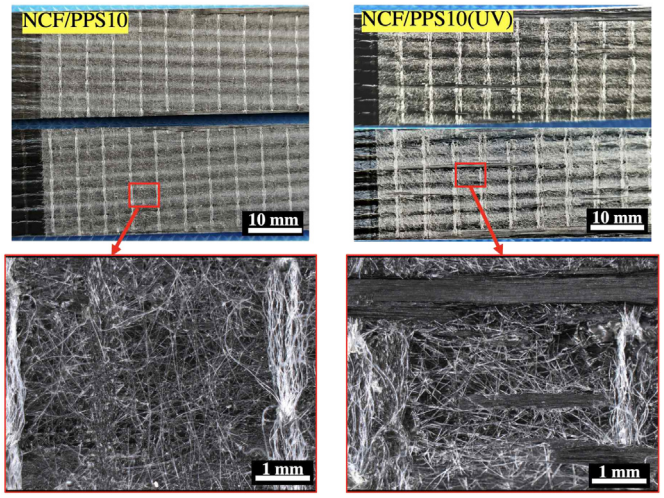

Fig. 3. Typical photographs and light microscopy images of the mode-I fracture surfaces of the NCF laminates.

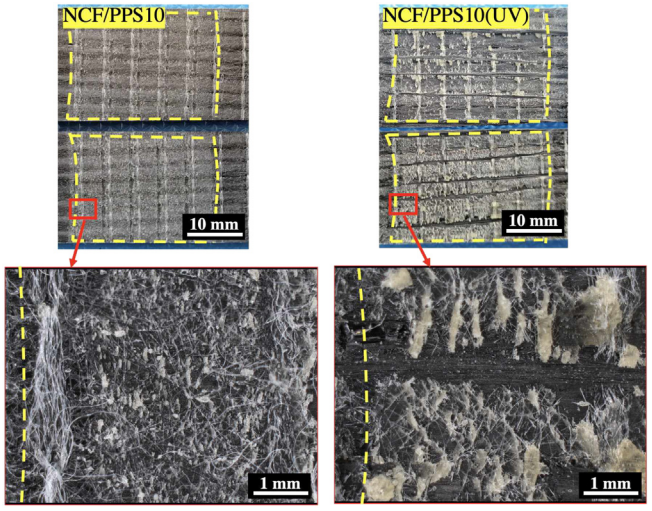

Fig. 5. Representative photographs and light microscopy images of the fracture surfaces of the ELS specimens of the NCF laminates.

The improved level of PPS fibre/epoxy adhesion also caused detrimental effects to the mode-II fracture behaviour of the interleaved UD laminates. Previous work [18] revealed that the addition of original PPS veils significantly improved the mode-II fracture toughness of the UD laminates, but also caused dynamic fracture of the ELS specimens after a short stable crack propagation of a few millimetres, as can be seen from the representative mode-II *R*-curves in Fig. 8. Applying the UV-treatment to the PPS veils further reduced the stability of the crack propagation in the ELS specimens, i.e. the entire specimens immediately failed dynamically once the crack started to propagate, referring to only one point on the corresponding *R*-curves in Fig. 8. The mode-II fracture energies of the UD laminates are summarised in Table 3. Both G_{IIC}^{ini} and G_{IIC}^{prop} considerably dropped upon the UV-treatment, i.e. G_{IIC}^{prop} decreased from around 2000 J/m^2 for the UD/PPS laminates to around 1100 J/m^2 for the UD/PPS(UV) laminates, as shown in Fig. 8 and Table 3. Moreover, no fibre bridging took place for the UD laminates containing UV-treated veils due to the dynamic failure of the entire ELS specimens, and the corresponding ΔG_{IIC} was essentially zero. Fig. 9 presents representative photographs and light microscopy images of the fracture surfaces of the ELS specimens of the UD laminates. The yellow dashed lines indicate the fronts of the pre-cracks, those were generated by applying an opening load to the specimens. For the UD/PPS10 laminate, the crack propagated cohesively in the PPS veils/epoxy layer during the stable crack propagation state of the ELS specimens, leaving most the PPS fibres on the upper surface and the rest of them on the lower surface, see Fig. 9. The improved veil/epoxy adhesion upon the UV-treatment enhanced the fracture resistance of the veil/epoxy layer, and consequently alternated the failure mode from a cohesive failure for the UD/PPS10 laminate to an interfacial failure between the veil/epoxy layer and the carbon fibres for the UD/PPS10(UV) laminates.

3.4. Toughening mechanisms and discussion

Sections 3.2 and 3.3 showed that applying the UV-treatment to the PPS veils significantly enhanced their toughening performance for the NCF laminates, and caused considerable deteriorations in the fracture behaviour of the interleaved UD laminates. In this section, the fracture mechanisms of the interleaved laminates were investigated to understand the reasons for causing the significantly varied toughening performance of the PPS veils for different laminate systems. Representative SEM images of the mode-I and mode-II fracture surfaces of the interleaved NCF laminates are shown in Fig. 10. As shown in Fig. 10(a) and (b), a large number of pulled-out PPS fibres in a long and continuous form existed on both of the mode-I and mode-II fracture surfaces of the NCF/PPS10 laminate, indicating the presence of extensive PPS fibre bridging during the fracture process. Additionally, no evidence of damage to these PPS fibres themselves was observed, see Fig. 10(c) and (d). In contrast, almost all the pulled-out PPS fibres on the mode-I and mode-II fracture surfaces of the NCF/PPS10(UV) laminate possessed relatively short free edges, with the main section of the PPS fibres embedded in the epoxy matrix, as shown in Fig. 10(e) and (f). Moreover, Fig. 10(g) and (h) shows that the free edges of the pulled-out PPS fibres

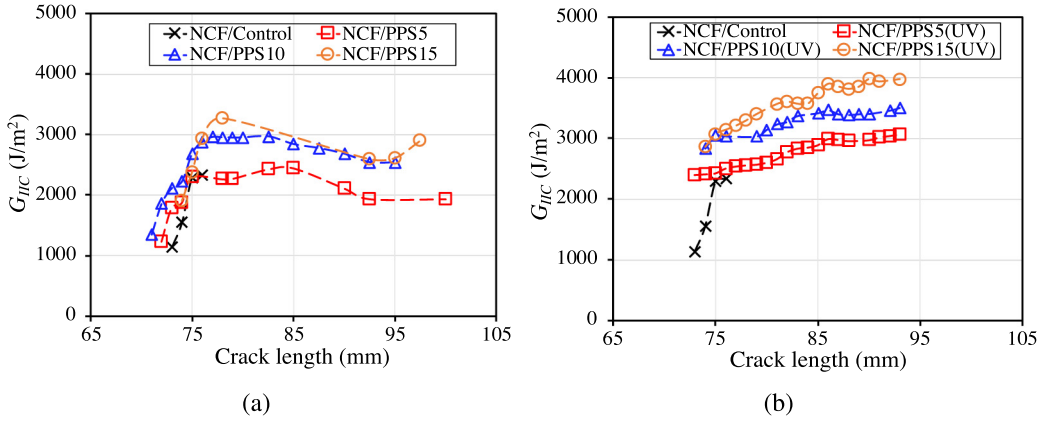

Fig. 4. Representative mode-II *R*-curves of the NCF laminates interleaved with (a) original [18] and (b) UV-treated PPS veils from the ELS tests.

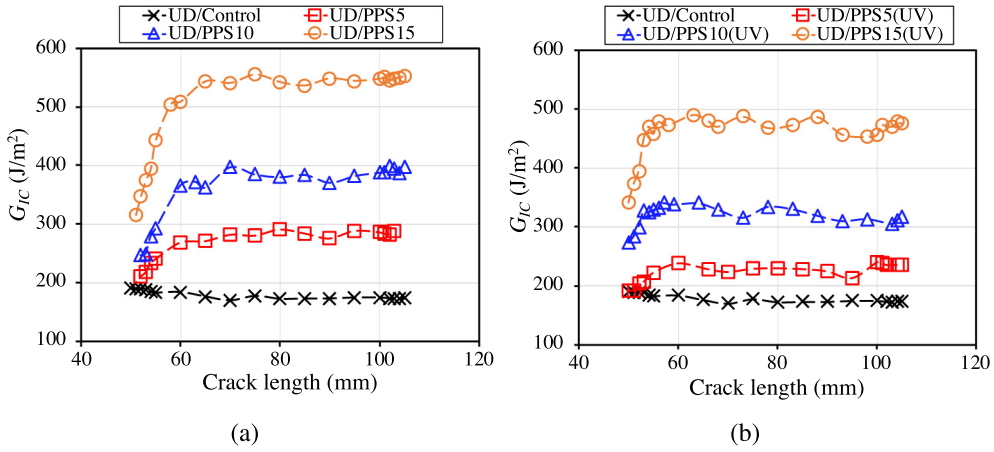

Fig. 6. Representative mode-I *R*-curves of the UD laminates interleaved with (a) original [19] and (b) UV-treated PPS veils.

were significantly damaged during the fracture process of the NCF/PPS10(UV) laminates. These phenomena indicate extensive plastic deformation and breakage of the PPS fibres during the fracture process of the laminates, and clearly demonstrated an improved PPS fibre/epoxy adhesion upon performing the UV-treatment to the PPS veils. In conclusion, the application of the UV-treatment to the PPS veils increased the veil/epoxy adhesion, and subsequently resulted in additional carbon fibre delamination (as shown in Figs. 3 and 5) and severe damage to the thermoplastic fibres during the fracture process of the NCF laminates. These mechanisms improved the toughening performance of the PPS veils for the NCF laminates. However, the improved veil/epoxy adhesion also restrained the PPS fibre bridging mechanism during the fracture process, evidenced by the absence of long and continuous pulled-out PPS fibres in Fig. 10(e) and (f). This led to the decreases in ΔG_{IC} and ΔG_{IIC} in Table 2. It should be noted that not all the PPS fibres had been actively involved in the laminate toughening for the mode-I fracture of both the NCF/PPS10 and the NCF/PPS10(UV) laminates. As may be clearly seen from Fig. 10(a) and (e), many of the PPS fibres were still well-attached to the epoxy matrix, exhibiting no fibre pulling-out and bridging for the NCF/PPS10 laminate and no obvious fibre damage for the NCFPPS10(UV) laminates. A quantitative examination of the fracture surfaces based on the SEM images revealed that approximately 62% of the PPS fibres pulled-out and bridged the crack during the fracture process of the NCF/PPS10 laminate, and approximately 30% of the UV-treated PPS fibres exhibited obvious damage during the fracture process of the NCF/PPS10(UV) laminates. Obviously, a smaller proportion of PPS fibres contributed to the toughening mechanisms of the UV-treated PPS veils, that resulted in a less prominent effect of their areal density on G_{IC}^{prop} of the NCF laminates, as shown in Table 2. A decrease in the number of active PPS fibres for toughening, together with a reduction in the amount PPS fibre bridging upon the UV-treatment could negatively affect the mode-I fracture behaviour of the NCF laminates. This explained why G_{IC}^{prop} of the NCF/PPS15(UV) laminate was slightly lower than that of the NCF/PPS15 laminate, see Table 2.

Fig. 11 presents representative SEM images of the fracture surfaces of the interleaved UD laminates. Fig. 11(a) and (b) shows that the pulled-out PPS fibres on the mode-I and mode-II fracture surfaces of the UD/PPS10 laminate were in a long and continuous form, indicating significant PPS fibre bridging mechanism. On closer examination, no obvious damage to the PPS fibres themselves took place during the mode-I and mode-II fracture process of the UC/PPS10 laminate, as shown in Fig. 11(c) and (d). For the UD/PPS10(UV) laminate, most of the pulled-out PPS fibres were relatively short with the majority section of the fibres embedded in the epoxy matrix on the mode-I fracture surfaces (see Fig. 11(e)), and all the PPS fibres were embedded in the epoxy matrix on the mode-II fracture surfaces (see Fig. 11(f)). Theses phenomena demonstrated that the improved veil/epoxy adhesion inhibited the debonding of the PPS fibres from the matrix, that considerably reduced the amount of PPS fibre bridging during the fracture process of the UD/PPS10(UV) laminates and led to the decreases in the values of ΔG_{IC} and ΔG_{IIC} in Table 3. Moreover, unlike the counterparts of the NCF laminates, no evidence of obvious damage to the PPS fibres themselves was observed for the UD laminates interleaved with UV-treated veils, as shown in Fig. 11(g) and (h). Overall, the application of the UV-treatment to the PPS veils restrained the PPS fibre bridging mechanism (without introducing PPS fibre damage mechanisms) during the fracture process of the interleaved UD laminates, that consequently led to significant deteriorations to the mode-I and mode-II fracture energies, see Table 3. These observations agreed well with our previous work [17,38].

It remains to be answered, why an improved PPS veil/epoxy adhesion resulted in different fracture mechanisms for the interleaved UD and NCF laminates. This was very likely attributed to two factors; 1) the different levels of adhesion at the UV-treated PPS veils/epoxy

Table 3
The mode-I and mode-II fracture energies of the interleaved UD laminates. $\Delta G = G^{prop} - G^{ini}$. The symbol '≈' means no statistical difference between G_{IC}^{ini} and G_{IC}^{prop}. Values in brackets indicate the percentage increases of the fracture energies over those of the corresponding control laminates.

Specimens	G_{IC}^{ini} (J/m^2)	G_{IC}^{prop} (J/m^2)	ΔG_{IC} (J/m^2)	G_{IIC}^{ini} (J/m^2)	G_{IIC}^{prop} (J/m^2)	ΔG_{IIC} (J/m^2)
UD control	181 ± 9	171 ± 8	≈	627 ± 22	630 ± 26	≈
Original PPS veils						
UD/PPS5	210 ± 27 (16%)	282 ± 2 (65%)	72	1654 ± 178 (162%)	1939 ± 101 (209%)	285
UD/PPS10	243 ± 9 (34%)	368 ± 44 (115%)	125	1783 ± 46 (183%)	2128 ± 57 (240%)	345
UD/PPS15	316 ± 27 (74%)	542 ± 42 (216%)	226	1807 ± 228 (187%)	2053 ± 77 (228%)	246
UV-treated PPS veils						
UD/PPS5(UV)	196 ± 8 (8%)	222 ± 16 (30%)	26	1118 ± 56 (77%)	1134 ± 68 (81%)	≈
UD/PPS10(UV)	259 ± 8 (43%)	317 ± 10 (85%)	58	1258 ± 118 (100%)	1264 ± 123 (102%)	≈
UD/PPS15(UV)	356 ± 14 (97%)	471 ± 37 (175%)	115	1030 ± 126 (63%)	1029 ± 87 (64%)	≈

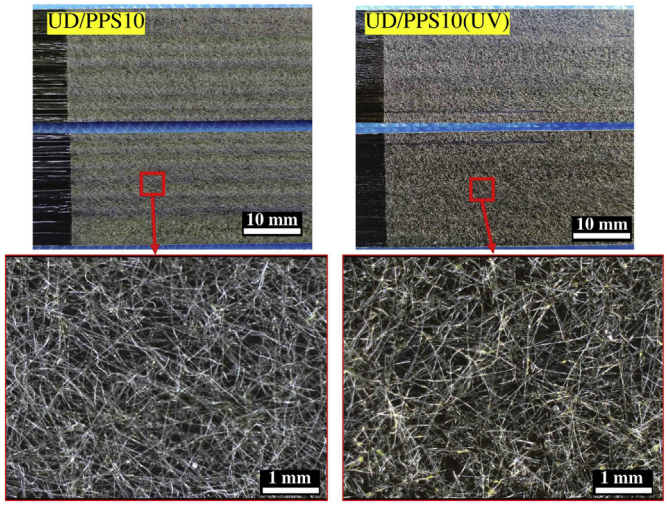

Fig. 7. Representative photographs and light microscopy images of the fracture surfaces of the DCB specimens of the UD laminates.

interface and 2) the different levels of adhesion between the carbon fibres and the epoxy matrix within the UD and NCF laminates. Firstly, the adhesion between the UV-treated PPS veils and the epoxy matrix was relatively higher within the interleaved NCF laminates than that within the UD laminates. Fig. 10(g) shows that the adhesion between the UV-treated PPS fibres and the epoxy matrix of the NCF laminate was sufficient to cause severe damage to the PPS fibres themselves during the mode-I fracture process. However, under the same circumstances, the PPS fibre/epoxy adhesion within the UD laminates was only able to inhibit debonding and pull-out of the UV-treated PPS fibres, without causing obvious damage to the PPS fibres, as shown in Fig. 11(g). Secondly, the adhesion between the carbon fibres and the epoxy matrix also appeared to be relatively higher for the NCF laminate than that for the UD laminates, based the following phenomena. The mode-II crack propagated purely interfacially between the veil/epoxy layer and the carbon fibres for the UD/PPS10(UV) laminate, leaving a very smooth surface of the veil/epoxy layer on the upper fracture surface in Fig. 9. Nevertheless, for the NCF/PPS(10) laminates, a large number of fractured epoxy debris and PPS fibres, together with carbon fibre delamination were observed on both sides of the mode-II fracture surfaces, as shown in Fig. 5. It means that, in this case, the adhesion at the carbon fibre/epoxy interface was sufficiently high to cause damage to both the carbon fibre side and the epoxy/veil side materials. It is worthy noting that the compatibility of the epoxy matrix with the thermoplastic veils and the carbon fibres can be affected by the surface activity of the thermoplastic veils and the carbon fibres, the formulation of the epoxy monomers and the laminate processing method, i.e. prepreg or RTM [19]. Unfortunately,

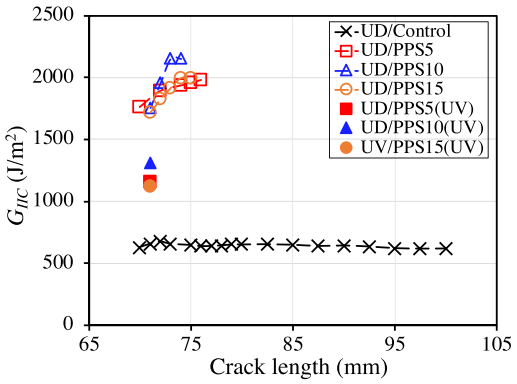

Fig. 8. Representative mode-II *R*-curves from the ELS tests of the UD laminates.

detailed information on the adhesion property of the epoxy resins and the surface treatment procedure of the carbon fibres was not available as this remains proprietary information of the suppliers. However, both the UD and NCF laminates studied were verified aerospace-grade systems, and hence, the epoxy resins should have been functionalised and the surface of the carbon fibres should have been properly treated to ensure a sufficient adhesion between them. Accordingly, the significant differences in the toughening levels of the UV-treated PPS veils for the UD and NCF laminates were very likely due to the different laminate processing methods, i.e. prepreg for the UD laminates, and RTM for the NCF laminates. The epoxy resin used for the RTM of the NCF laminates was in form of low molecular weight monomers having low viscosity and high flowability for easy processing. However, the epoxy in the UD prepreg was partially cured during the impregnation process, i.e. at a B-stage of curing. The advantage of B-stage epoxies is that they are at an intermediate level of cure providing the epoxy with film-like properties for easy handling and storage of the prepreg [39]. Nevertheless, the B-staging process reduced the flowability of the epoxy resin of the UD prepreg, that could negatively affect the compatibility between the thermoplastic fibres and the epoxy. Moreover, it could also reduce the quantity of reactive groups in the the epoxy system to covalently bond to the functional groups of the U-treated PPS surface, and also tends to affect the adhesion between the epoxy and the carbon fibres. This may explain why the UD laminates exhibited relatively lower level of epoxy/fibre adhesion than the NCF laminates.

4. Conclusions

A UV-irradiation technique was proposed to active the surfaces of PPS veils, aiming to improve the veil/epoxy adhesion in CFRPs interleaved by PPS veils. A chemical characterisation of the non-treated and UV-treated PPS surfaces demonstrated that applying a 10 s UV-treatment notably increased the level of the oxygen elements on the PPS surfaces. This subsequently improved the wettability of the PPS surfaces, i.e. the water contact angles decreased from 79.7 ± 1.9° to 43.0 ± 0.8°. The UV-irradiation had been proven to effectively enhance the veil/epoxy adhesion. Consequently, it offers the possibility to carry out comprehensive characterisations of the interleaved laminates with improved veil/epoxy adhesion, and subsequently further develop advanced composite materials.

In this work, the fracture behaviour of aerospace-grade CFRPs interleaved with PPS veils was studied, with the veil/epoxy adhesion significantly improved upon applying the UV-treatment to the PPS veils. Two laminate systems manufactured by unidirectional (UD) prepregs and resin transfer moulding of non-crimp fabrics (NCF) were studied in this paper, as they exhibited significantly different fracture energies and mechanisms. The different fracture behaviour and mechanisms of the non-modified laminates resulted in significantly different toughening performance of the UV-treated PPS veils. For the NCF laminates, applying the UV-treatment to the PPS veils resulted in additional significant carbon fibre delamination and PPS fibre damage during the fracture process, and subsequently led to remarkable increases in the mode-I and mode-II fracture energies. For the UD laminates, no evidence of carbon fibre delamination and PPS fibre damages was observed on the fracture surfaces. Additionally, the enhanced PPS veil/epoxy adhesion upon the UV-treatment inhibited the PPS fibre bridging (the main toughening mechanisms of the original PPS veils) during the fracture process, and subsequently caused deteriorations in the fracture behaviour of the laminates. Overall, this work revealed obvious effects of the veil/epoxy adhesion on the fracture behaviour of interleaved laminates, and moreover, these effects significantly varied in different CFRP systems. Declaration of competing interest

We declare that we have no financial and personal relationships with other people or organizations that can inappropriately influence our work, there is no professional or other personal interest of any nature or kind in any product, service and/or company that could be

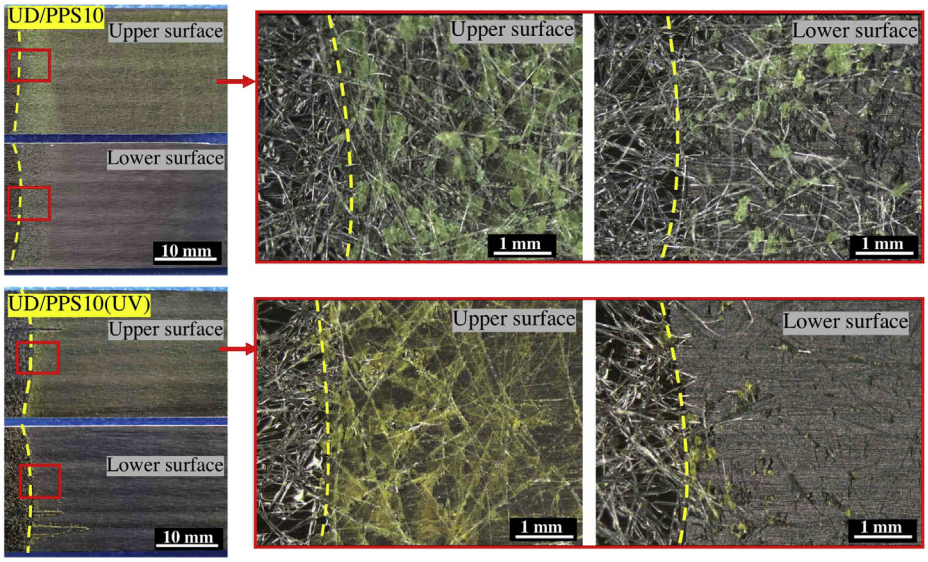

Fig. 9. Representative photographs and light microscopy images of the fracture surfaces of the ELS specimens of the UD laminates. The yellow dashed lines indicate the fronts of the pre-cracks. The red colour boxes in the photographs indicate the areas imaged by the light microscope. (For interpretation of the references to colour in this figure legend, the reader is referred to the web version of this article.)

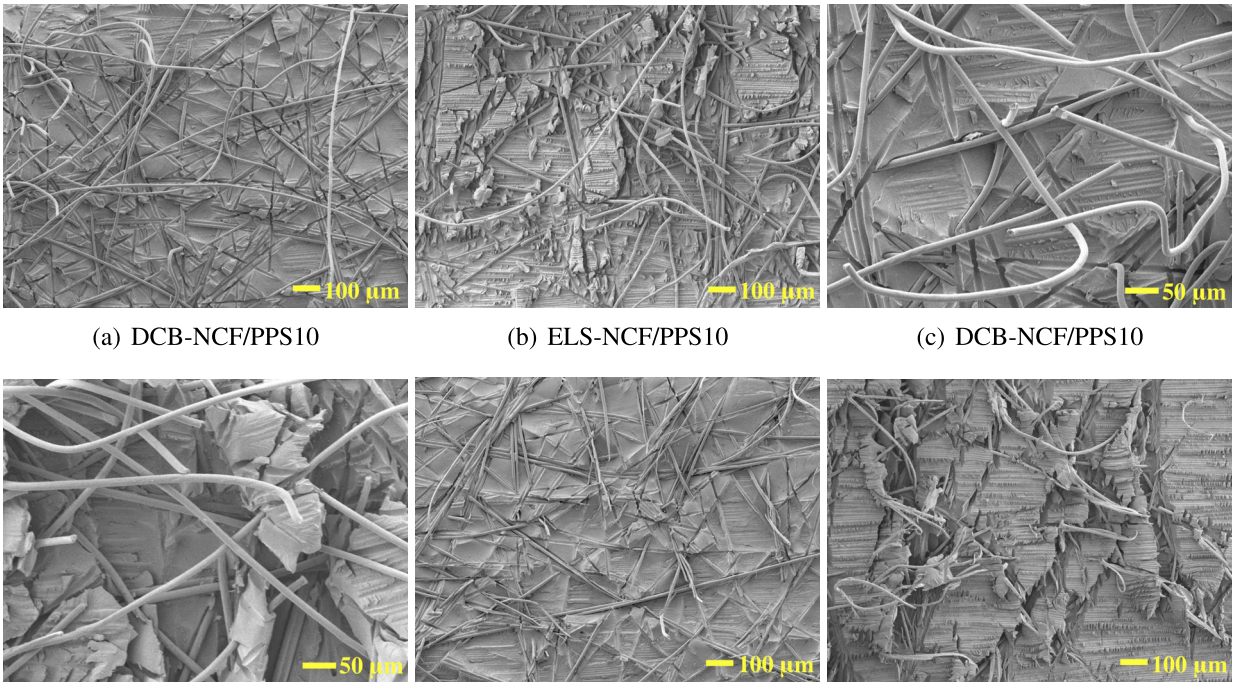

(a) DCB-NCF/PPS10 (b) ELS-NCF/PPS10 (c) DCB-NCF/PPS10

(d) ELS-NCF/PPS10 (e) DCB-NCF/PPS10(UV) (f) ELS-NCF/PPS10(UV)

(g) DCB-NCF/PPS10(UV) (h) ELS-NCF/PPS10(UV)

Fig. 10. Representative SEM images of the mode-I and mode-II fracture surfaces of the interleaved NCF laminates.

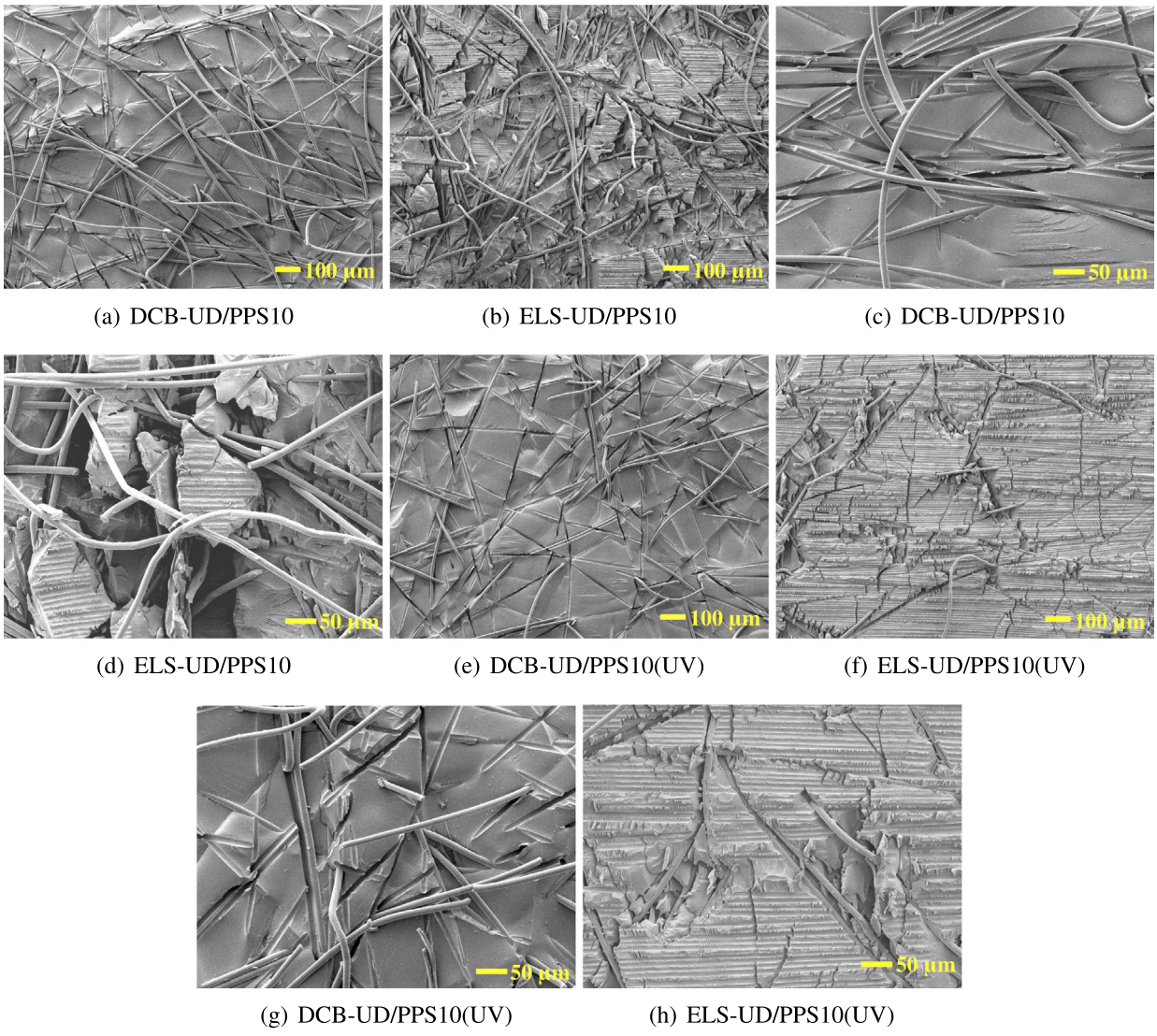

Fig. 11. Representative SEM images of the mode-I and mode-II fracture surfaces of the interleaved UD laminates.

construed as influencing the position presented in, or the review of, the manuscript entitled, "The influence of interlayer/epoxy adhesion on the Mode-I and Mode-II fracture response of carbon fibre/epoxy composites interleaved with thermoplastic veils".

CRediT authorship contribution statement

Dong Quan: Investigation, Writing - original draft, Funding acquisition.**Brian Deegan:**Methodology, Validation, Resources.**René Alderliesten:**Investigation, Supervision, Funding acquisition, Project administration, Writing - review & editing.**Clemens Dransfeld:**Methodology, Writing - review & editing.**Neal Murphy:**Resources, Validation, Funding acquisition.**Alojz Ivanković:**Methodology, Resources, Funding acquisition.**Rinze Benedictus:**Resources, Supervision, Funding acquisition.

Acknowledgements

This work is funded by the European Union's Horizon 2020 research and innovation programme under the Marie Skłodowska-Curie grant agreement No. 842467. Financial support from the Irish Composites Centre is also acknowledged. We would like to thank Bombardier Aerospace (UK) and Technical Fibre Products (UK) for supplying the carbon fibre fabrics and thermoplastic veils.

Data availability

The raw/processed data required to reproduce these findings cannot be shared at this time due to legal or ethical reasons.

References

[1] R. Palazzetti, A. Zucchelli, Electrospun nanofibers as reinforcement for composite laminates materials—a review, Compos. Struct. 182 (2017) 711–727, https://doi.org/10.1016/j.compstruct.2017.09.021.
[2] B. Beylergil, M. Tanoglu, E. Aktas, Enhancement of interlaminar fracture toughness of carbon fiber/epoxy composites using polyamide-6,6 electrospun nanofibers, J. Appl. Polym. Sci. 134 (35) (2017) 45244, https://doi.org/10.1002/app.45244.
[3] B. Beylergil, M. Tanoglu, E. Aktas, Effect of polyamide-6,6 (PA 66) nonwoven veils on the mechanical performance of carbon fiber/epoxy composites, Compos. Struct. 194 (2018) 21–35, https://doi.org/10.1016/j.compstruct.2018.03.097.
[4] B. Beylergil, M. Tanoglu, E. Aktas, Mode-I fracture toughness of carbon fiber/epoxy composites interleaved by aramid nonwoven veils, Steel Compos. Struct. 31 (2) (2019) 113–123, https://doi.org/10.12989/scs.2019.31.2.113.
[5] R. Palazzetti, A. Zucchelli, C. Gualandi, M. Focarete, L. Donati, G. Minak, S. Ramakrishna, Influence of electrospun nylon 6,6 nanofibrous mats on the interlaminar properties of Gr-epoxy composite laminates, Compos. Struct. 94 (2) (2012) 571–579, https://doi.org/10.1016/j.compstruct.2011.08.019.

[6] R. Palazzetti, A. Zucchelli, I. Trendafilova, The self-reinforcing effect of Nylon 6,6 nano-fibres on CFRP laminates subjected to low velocity impact, Compos. Struct. 106 (2013) 661–671, https://doi.org/10.1016/j.compstruct.2013.07.021.
[7] H. Saghafi, A. Zucchelli, R. Palazzetti, G. Minak, The effect of interleaved composite nanofibrous mats on delamination behavior of polymeric composite materials, Compos. Struct. 109 (2014) 41–47, https://doi.org/10.1016/j.compstruct.2013.10.039.
[8] T. Brugo, R. Palazzetti, The effect of thickness of Nylon 6,6 nanofibrous mat on Modes I–II fracture mechanics of UD and woven composite laminates, Compos. Struct. 154 (2016) 172–178, https://doi.org/10.1016/j.compstruct.2016.07.034.
[9] D.W. Wong, L. Lin, P.T. McGrail, T. Peijs, P.J. Hogg, Improved fracture toughness of carbon fibre/epoxy composite laminates using dissolvable thermoplastic fibres, Compos. A: Appl. Sci. Manuf. 41 (6) (2010) 759–767, https://doi.org/10.1016/j.compositesa.2010.02.008.
[10] L.M.K. Molnar, E. Kostakova, The effect of needleless electrospun nanofibrous interleaves on mechanical properties of carbon fabrics/epoxy laminates, Express Polym Lett 8 (1) (2014) 62–72, https://doi.org/10.3144/expresspolymlett.2014.8.
[11] B. Beylergil, M. Tanoglu, E. Aktas, Modification of carbon fibre/epoxy composites by polyvinyl alcohol (PVA) based electrospun nanofibres, Adv. Compos. Lett. 25 (3) (2016) 69–76, https://doi.org/10.1177/096369351602500303.
[12] G.W. Beckermann, K.L. Pickering, Mode I and Mode II interlaminar fracture toughness of composite laminates interleaved with electrospun nanofibre veils, Compos. A: Appl. Sci. Manuf. 72 (2015) 11–21, https://doi.org/10.1016/j.compositesa.2015.01.028.
[13] G.W. Beckermann, Nanofiber interleaving veils for improving the performance of composite laminates, Reinf. Plast. 61 (5) (2017) 289–293, https://doi.org/10.1016/j.repl.2017.03.006.
[14] L. Daelemans, S. van der Heijden, I.D. Baere, H. Rahier, W.V. Paepegem, K.D. Clerck, Nanofibre bridging as a toughening mechanism in carbon/epoxy composite laminates interleaved with electrospun polyamide nanofibrous veils, Compos. Sci. Technol. 117 (2015) 244–256, https://doi.org/10.1016/j.compscitech.2015.06.021.
[15] M. Kuwata, P. Hogg, Interlaminar toughness of interleaved CFRP using non-woven veils: part 1. Mode-I testing, Compos. A: Appl. Sci. Manuf. 42 (10) (2011) 1551–1559, https://doi.org/10.1016/j.compositesa.2011.07.016.
[16] M. Kuwata, P. Hogg, Interlaminar toughness of interleaved CFRP using non-woven veils: part 2. Mode-II testing, Compos. A: Appl. Sci. Manuf. 42 (10) (2011) 1560–1570, https://doi.org/10.1016/j.compositesa.2011.07.017.
[17] D. Quan, C. Mischo, L. Binsfeld, A. Ivankovic, N. Murphy, Fracture behaviour of carbon fibre/epoxy composites interleaved by MWCNT- and graphene nanoplatelet-doped thermoplastic veils, Compos. Struct. (2019) 111767, https://doi.org/10.1016/j.compstruct.2019.111767.
[18] D. Quan, F. Bologna, G. Scarselli, A. Ivankovic, N. Murphy, Mode-II fracture behaviour of aerospace-grade carbon fibre/epoxy composites interleaved with thermoplastic veils, Compos. Sci. Technol. 191 (2020), 108065. https://doi.org/10.1016/j.compscitech.2020.108065.
[19] D. Quan, F. Bologna, G. Scarselli, A. Ivankovic, N. Murphy, Interlaminar fracture toughness of aerospace-grade carbon fibre reinforced plastics interleaved with thermoplastic veils, Compos. A: Appl. Sci. Manuf. 128 (2020), 105642. https://doi.org/10.1016/j.compositesa.2019.105642.
[20] G. Li, P. Li, C. Zhang, Y. Yu, H. Liu, S. Zhang, X. Jia, X. Yang, Z. Xue, S. Ryu, Inhomogeneous toughening of carbon fiber/epoxy composite using electrospun polysulfone nanofibrous membranes by in situ phase separation, Compos. Sci. Technol. 68 (3) (2008) 987–994, https://doi.org/10.1016/j.compscitech.2007.07.010.
[21] L. Daelemans, S. van der Heijden, I. De Baere, H. Rahier, W. Van Paepegem, K. De Clerck, Damage-resistant composites using electrospun nanofibers: a multiscale analysis of the toughening mechanisms, ACS Appl. Mater. Interfaces 8 (18) (2016) 11806–11818, https://doi.org/10.1021/acsami.6b02247.
[22] L. Daelemans, S. van der Heijden, I.D. Baere, H. Rahier, W.V. Paepegem, K.D. Clerck, Improved fatigue delamination behaviour of composite laminates with electrospun thermoplastic nanofibrous interleaves using the Central Cut-Ply method, Compos. A: Appl. Sci. Manuf. 94 (2017) 10–20, https://doi.org/10.1016/j.compositesa.2016.12.004.
[23] A.J. Kinloch, G.K.A. Kodokian, J.F. Watts, Relationships between the surface free energies and surface chemical compositions of thermoplastic fibre composites and adhesive joint strengths, J. Mater. Sci. Lett. 10 (14) (1991) 815–818, https://doi.org/10.1007/BF00724747.
[24] K. O'Donovan, D. Ray, M.A. McCarthy, Toughening effects of interleaved nylon veils on glass fabric/low-styrene-emission unsaturated polyester resin composites, J. Appl. Polym. Sci. 132 (7) (2015) 41462, https://doi.org/10.1002/app.41462.
[25] B. Del Saz-Orozco, D. Ray, W.F. Stanley, Effect of thermoplastic veils on interlaminar fracture toughness of a glass fiber/vinyl ester composite, Polym. Compos. 38 (11) (2017) 2501–2508, https://doi.org/10.1002/pc.23840.
[26] N. Nash, D. Ray, T. Young, W. Stanley, The influence of hydrothermal conditioning on the mode-i, thermal and flexural properties of carbon/benzoxazine composites with a thermoplastic toughening interlayer, Compos. A: Appl. Sci. Manuf. 76 (2015) 135–144, https://doi.org/10.1016/j.compositesa.2015.04.023.
[27] D.A. Bolon, C.O. Kunz, Ultraviolet depolymerization of photoresist polymers, Polym. Eng. Sci. 12 (2) (1972) 109–111, https://doi.org/10.1002/pen.760120206.
[28] S. Bok, G.-H. Lim, B. Lim, UV/ozone treatment for adhesion improvement of copper/epoxy interface, J. Ind. Eng. Chem. 46 (2017) 199–202, https://doi.org/10.1016/j.jiec.2016.10.031.
[29] J. Liu, L. He, L. Wang, Y. Man, L. Huang, Z. Xu, D. Ge, J. Li, C. Liu, L. Wang, Significant enhancement of the adhesion between metal films and polymer substrates by UV–ozone surface modification in nanoscale, ACS Appl. Mater. Interfaces 8 (44) (2016) 30576–30582, https://doi.org/10.1021/acsami.6b09930.
[30] H. Le-The, R.M. Tiggelaar, E. Berenschot, A. van den Berg, N. Tas, J.C.T. Eijkel, Postdeposition UV-ozone treatment: an enabling technique to enhance the direct adhesion of gold thin films to oxidized silicon, ACS Nano 13 (6) (2019) 6782–6789, https://doi.org/10.1021/acsnano.9b01403.
[31] H. Shi, J. Sinke, R. Benedictus, Surface modification of PEEK by UV irradiation for direct co-curing with carbon fibre reinforced epoxy prepregs, Int. J. Adhes. Adhes. 73 (2017) 51–57, https://doi.org/10.1016/j.ijadhadh.2016.07.017.
[32] BS ISO 15024:2001, Fibre-reinforced Plastic Composites Determination of Mode I Interlaminar Fracture Toughness, G^{IC} for Unidirectionally Reinforced Materials, 2001.
[33] ISO 15114:2014, Fibre-reinforced Plastic Composites Determination of Mode II Fracture Resistance for Unidirectionally Reinforced Materials Using the Calibrated End-loaded Split (C-ELS) Test and an Effective Crack Length Approach, 2014.
[34] G.K.A. Kodokian, A.J. Kinloch, The adhesive fracture energy of bonded thermoplastic fibre-composites, J. Adhes. 29 (1–4) (1989) 193–218, https://doi.org/10.1080/00218468908026487.
[35] A.J. Kinloch, G.K.A. Kodokian, J.F. Watts, The adhesion of thermoplastic fibre composites, Philos. Trans. R. Soc. Lond. Ser A Phys. Eng. Sci. 338 (1649) (1992) 83–112, https://doi.org/10.1098/rsta.1992.0004.
[36] I. Mathieson, R. Bradley, Improved adhesion to polymers by UV/ozone surface oxidation, Int. J. Adhes. Adhes. 16 (1) (1996) 29–31, https://doi.org/10.1016/0143-7496(96)88482-X.
[37] B.F. Sorensen, T.K. Jacobsen, Large-scale bridging in composites: R-curves and bridging laws, Compos. A: Appl. Sci. Manuf. 29 (11) (1998) 1443–1451, https://doi.org/10.1016/S1359-835X(98)00025-6.
[38] D. Quan, C. Mischo, X. Li, G. Scarselli, A. Ivankovic, N. Murphy, Improving the electrical conductivity and fracture toughness of carbon fibre/epoxy composites by interleaving MWCNT-doped thermoplastic veils, Compos. Sci. Technol. 182 (2019), 107775. https://doi.org/10.1016/j.compscitech.2019.107775.
[39] S. Costantino, U. Waldvogel, Composite processing: state of the art and future trends, in: J.-P. Pascault, R.J.J.P. Williams (Eds.), Epoxy Polymers, John Wiley & Sons, Ltd 2010, pp. 275–277.